



Flood hazard mapping using a GIS-based morphometric analysis approach in arid regions, a case study in the Red Sea Region, Egypt

Ahmed G. Abdelgawad¹ · Esam Helal¹ · Mohmaed F. Sobeih¹ · Hamdy Elsayed^{1,2}

Received: 14 September 2023 / Accepted: 2 February 2024
© The Author(s) 2024

Abstract

Flash floods are a major threat to life and properties in arid regions. In recent decades, Egypt has experienced severe flash floods that have caused significant damage across the country, including the Red Sea region. The aim of this study is to map the flood hazards in flood-prone areas along the Red Sea region using a Geographic Information System (GIS)-based morphometric analysis approach. To evaluate the flood hazard degree, the adopted methodology considers various morphometric parameters such as basin area, slope, sinuosity index, shape factor, drainage intensity, circularity ratio, and curve number. GIS techniques were employed to delineate the watershed and the drainage network. The delineated watershed was used together with the digitized maps of soil and land use types to estimate the curve number and the morphometric parameters for each subbasin. The flood hazard degrees are calculated based on the considered morphometric parameters and distinguished based on a five-degree scale ranging from very low to very high. Results indicate that 47% of the study area has a very high flood hazard degree. Furthermore, morphometric analysis results align with the runoff results simulated by a hydrological model, where, for example, basins with a high to very high hazard degree exhibited high runoff. This suggests the influence of physical characteristics on the hydrological behavior of the watershed and further validates the morphometric analysis presented in this work. The results presented here can help policy planners and decision-makers develop appropriate measures to mitigate flash floods and achieve sustainable development in arid regions.

Keywords Flood hazard mapping · GIS-based morphometric analysis · Sustainable development goals · The Red Sea region

Introduction

Flash floods are one of the most weather-related natural disasters. They are potentially dangerous because they occur rapidly and unexpectedly after intense precipitation

events, often within minutes to a few hours. A flash flood may occur in particular geographical areas characterized by steep hillsides, impermeable shallow soils, and exposed bare rock (Elsayad 2013). In such areas, drainage channels may prove inadequate to accommodate excessive runoff of such heavy rainfall events, leading to damaging floods. Floods could pose significant negative impacts on human and environmental systems (Amaechina et al. 2022; Manzoor et al. 2022). Despite their negative impacts, flash floods could have several positive aspects and contribute to sustainable development by various means in many regions. For instance, flash floods can recharge groundwater aquifers, thus increasing water availability in regions with limited water supply, such as Egypt (Al-Qudah 2011). To address the water scarcity challenges in Egypt, rainwater utilization is incorporated into the national water resources policy of 2037 as a policy measure to increase water supply in regions without access to Nile water, e.g., coastal areas (Ministry of Water Resources and Irrigation 2017; Gabr et al. 2023).

✉ Hamdy Elsayed
h.a.a.elsayed@uu.nl;
hamdy.abdelwahed@sh-eng.menofia.edu.eg

Ahmed G. Abdelgawad
aga.abdelgawad@sh-eng.menofia.edu.eg

Esam Helal
Esamhelal@sh-eng.menofia.edu.eg

Mohmaed F. Sobeih
sobeih@yahoo.com

¹ Civil Engineering Department, Faculty of Engineering, Menoufia University, Shebin El-Kom, Egypt

² Department of Earth Sciences, Faculty of Geosciences, Utrecht University, Utrecht, The Netherlands

Embracing such sustainable practices can thus enhance community resilience and minimize flood impacts. Therefore, it is essential to explore potential hazards associated with flash floods to develop targeted strategies and inform the decision-making process.

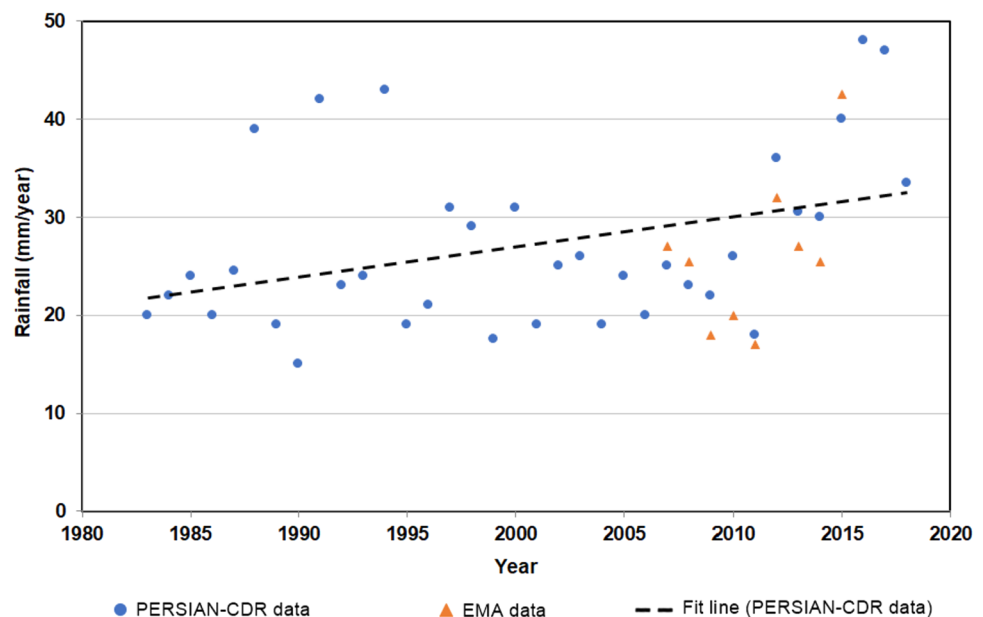
In Egypt, country-wide annual rainfall patterns indicate an increasing trend, as shown in Fig. 1 (Central Agency for Public Mobilization and Statistics 2015; National Centers for Environmental Information 2020; Saber et al. 2020). Over the past decades, Egypt has experienced severe flash floods (Saleh 2017) that have caused major losses to human lives, properties, and the economy. For instance, heavy flash floods in 1994 affected 124 villages and killed more than 600 people across four governorates in Upper Egypt (Moawad et al. 2016). Storm floods in 2010 caused substantial property damage, impacting 2000 houses in North Sinai. Moreover, a heavy rainfall event in October 2016 led to the loss of tens of people lives in Ras Gharib city, situated in the Red Sea Governorate (Moawad et al. 2016; Elnazer et al. 2017). The Red Sea coast region is currently experiencing an increasing trend in the frequency, severity, and impacts of heavy rainfall and flash flood events (Almasalmeh and Eizeldin 2020; Arnous et al. 2022). These severe flash floods pose significant threats to local communities, industrial facilities, and the tourism industry in the Red Sea region (Elnazer et al. 2017). Understanding and addressing flash floods is thus fundamental to reducing risks to livelihoods and protecting the environment, particularly in flood-prone regions such as the Red Sea region.

Flood hazard mapping approach is commonly applied to analyze floods risk and study flood characteristics such as depth and velocity of floodwater. Over the past decades, this approach has been significantly improved

and integrated into policy planning and decision-making processes in flood-prone regions (Mudashiru et al. 2021). For instance, the city of Houston, Texas, faced a severe flooding in 2017, resulted in numerous casualties and caused significant damage to infrastructure, residents, and businesses. In response to the disaster, the Harris County Flood Control District (HCFCD) initiated the development of a comprehensive flood hazard map. This map aimed to inform the public about flood risks, enabling them to take appropriate measures to safeguard themselves and their properties (Natsios 2018; Malecha et al. 2021; Harris County Flood Control District 2023).

Morphometric analysis is essential in studying catchment geomorphology (Sherief 2008). Estimating morphometric parameters for a basin holds a significant importance as these parameters govern its hydrological response and provide valuable insights into its hydrogeological characteristics. Therefore, studying morphometric analysis and understanding a basin's response to heavy rainfalls, storms, and floods are vital for effective flood risk analysis (Diakakis 2011; Cappelli et al. 2023). In data-scarce regions, morphometric properties of basins are commonly utilized to assess flood risks (Elsadek et al. 2019a). Flood hazard mapping, integrating morphometric analysis and geographic information systems (GIS), has emerged as a valuable tool for delineating and assessing the geohydrological properties of drainage basins (Mansour et al. 2023; Bogale 2021; Obeidat et al. 2021). For example, Omran et al. (2011) employed GIS techniques to generate flood hazard maps based on geomorphological parameters and to estimate flood risks in Wadi Dahab, Egypt. GIS techniques are instrumental in identifying flood risk zones and developing flood susceptibility maps. Moreover, they are promising tools as they can

Fig. 1 Annual rainfall estimates from the Precipitation Estimation from Remotely Sensed Information Using Artificial Neural Networks Climate Data Records (PERSIAN-CDR) satellite and the Egyptian Meteorological Authority (EMA) in Egypt



integrate multiple flood risk assessment methods through available features in GIS environments (Hagos et al. 2022).

Several studies have employed morphometric analysis to assess flood hazards. Youssef and Hegab (2019) utilized morphometric characteristics, geology maps, and hydrology data to determine flash flood susceptibility of watersheds within Ras Gharib area, Egypt. Their findings highlighted that three-quarters of the existing settlements are situated within high and very high susceptibility zones. Mashaly and Ghoneim (2018) incorporated morphometric parameters into a hydrological model to identify flood risk sites in the Red Sea region. Similarly, Mohamed et al. (2021) employed these methods to investigate the impact of hydrological parameters on flash floods in dry and semiarid regions like Wadi Al-Baroud El-Abiad in the Red Sea governorate, Egypt, by evaluating watershed morphometric characteristics. Taha et al. (2017) estimated morphometric parameters and implemented remote sensing techniques and GIS to evaluate flash flood hazards in the subbasins of Wadi Qena. Elsadek et al. (2019a) conducted a morphometric analysis of Wadi Qena watershed using GIS techniques, finding that about half of the subbasins exhibited hazard degrees ranging from moderate to high. Moreover, Mansour et al. (2023) employed morphometric analysis to map flash flood hazards for the Gulf of Suez in Egypt.

This study builds upon previous research methodologies to estimate flood hazards, particularly in data-scarce regions. While previous studies employed different methodologies and combinations of morphometric parameters for flood hazard analysis, this research employs a GIS-based analysis that is capable of rendering and processing large geospatial data, unlike conventional methods; thereby, GIS methods prove highly advantageous in data-limited regions (Bogale 2021; Hagos et al. 2022). The main aim of this study is to improve morphometric analysis in large-scale and data-scarce regions through the application of GIS techniques. To achieve this, a GIS-based framework was developed, incorporating a novel combination of morphometric parameters covering various watershed geomorphological characteristics such as area, shape, topography, and drainage network. Furthermore, the framework integrates the curve number as a runoff indicator, a less-addressed aspect in previous studies (Diakakis 2011; Taha et al. 2017; Hagos et al. 2022). The significance of the curve number lies in its role in representing rainfall-induced runoff during storm events (Ali et al. 2022; Lee et al. 2023). Moreover, an automated GIS model is developed to streamline GIS processes and expedite all GIS processes. This automation is particularly valuable in large-scale studies where handling multiple DEMs can be time-consuming and challenging (ArcGIS Pro 2023). Our framework provides flexibility in analyzing flood hazard degrees, adaptable to any combination of morphometric parameters and other regions. Finally, the developed framework is applied to a

study area located along the Red Sea coast, Egypt, spanning from Safaga to Port Ghalib, which remains unexplored at this large scale. The rest of the paper is organized as follows: (i) Study area description; (ii) Materials and methods; (iii) results and discussion; and (iv) Conclusion.

Study area description

The study area spans between Safaga and Port Ghalib, extending through Safaga in the Eastern Desert along the Red Sea coast of Upper Egypt, as shown in Fig. 2. It lies between longitudes 33.46° E to 34.49° E and latitudes 25.59° N to 27.09° N. The topography exhibits diverse characteristics, ranging from flat plains to steep mountains, with altitudes varying from -8 to 2,625 m above mean sea level. The study area encompasses critical infrastructure, tourist-centric cities, and economic activities. Major highways, such as the Hurghada-Safaga road and the Safaga-Quseir road, run almost parallel to the Red Sea coast, while rail networks traverse the lower reaches of most of the study area. The area also includes vital harbors, such as the Safaga harbor. Situated in the east-northeast of the study area, Safaga is renowned for its exquisite beaches and a wide array of tourist activities and medical tourism (The Red Sea Governorate 2023). Similarly, Quseir, a significant coastal city, is undergoing tourism development and is known for its historical significance (Mashaly and Ghoneim 2018). However, cities along the Red Sea coast, like Hurghada, Safaga, and Quseir, face heightened vulnerability to flash floods (Mohamed 2019).

The Red Sea region is prone to flash floods, with an annual probability of occurrence up to 20% (The World Bank Group 2021). Furthermore, the region is witnessing an increasing trend in rainfall intensity and frequency, with human and environmental impacts (Youssef et al. 2009). Specifically, severe flash floods have impacted the study area in recent decades, leading to profound consequences for human lives, livelihoods, and infrastructure (Sherief 2008; Elsadek et al. 2019b). For example, in October 1979, a severe flash flood struck the Red Sea Governorate, resulting in severe damages to the Quseir-Qena road, the destruction of 500 properties, and the deaths of 19 individuals. Subsequent floods affected the study area in 1980, 1985, 1989, 1991, and 1994 (Monsef 2018). The 1989 flood, triggered by heavy rain of 50 mm/day in Quseir, damaged the railway near the city, impacting the Quseir-Qena highway and the Quseir-Marsa Alam coastal highway (Monsef 2018). In October 1990, flash floods severely damaged the Qena-Safaga Railway, resulting in substructure failures totaling 21,000 m³, damage to three kilometers of the superstructure, two station buildings, and four signal towers (Abuzeid et al. 2022). The 1994 flash flood caused road damage in

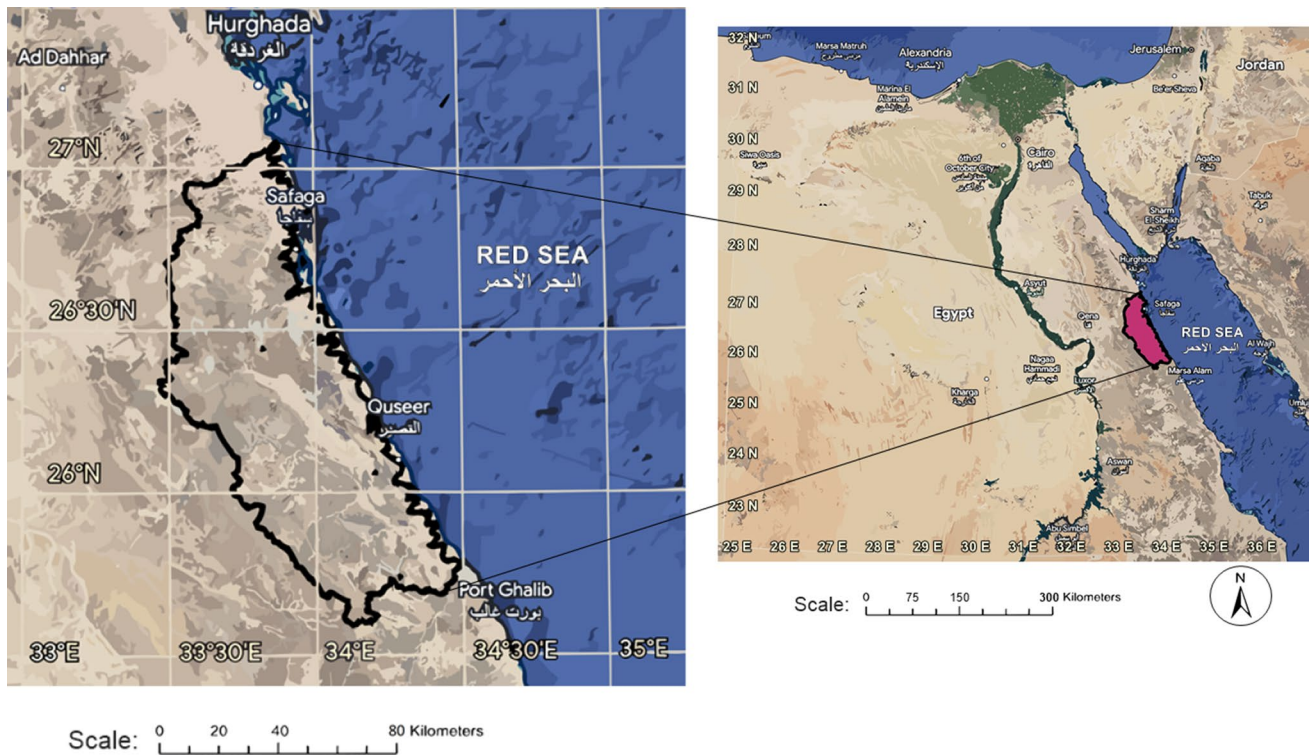


Fig. 2 Map of Egypt and the study area location

Quseir and damage to numerous buildings between Safaga and Quseir. Subsequent flood events, such as heavy rains in January 2010, disrupted traffic, caused casualties, and forced the closure of the Quseir-Qena highway for two days. Moreover, in May 2014, heavy rains hit the Red Sea Governorate, including the area between Safaga and Quseir, resulting in the destruction of 14 homes, road blockages, and blackouts (Monsef 2018). In September 2020, the Red Sea coast was struck with floods after heavy rain. This prompted closures on several highways in the area, including the Qift-Quseir road and the Safaga-Sohag road (Egypt Today staff 2020).

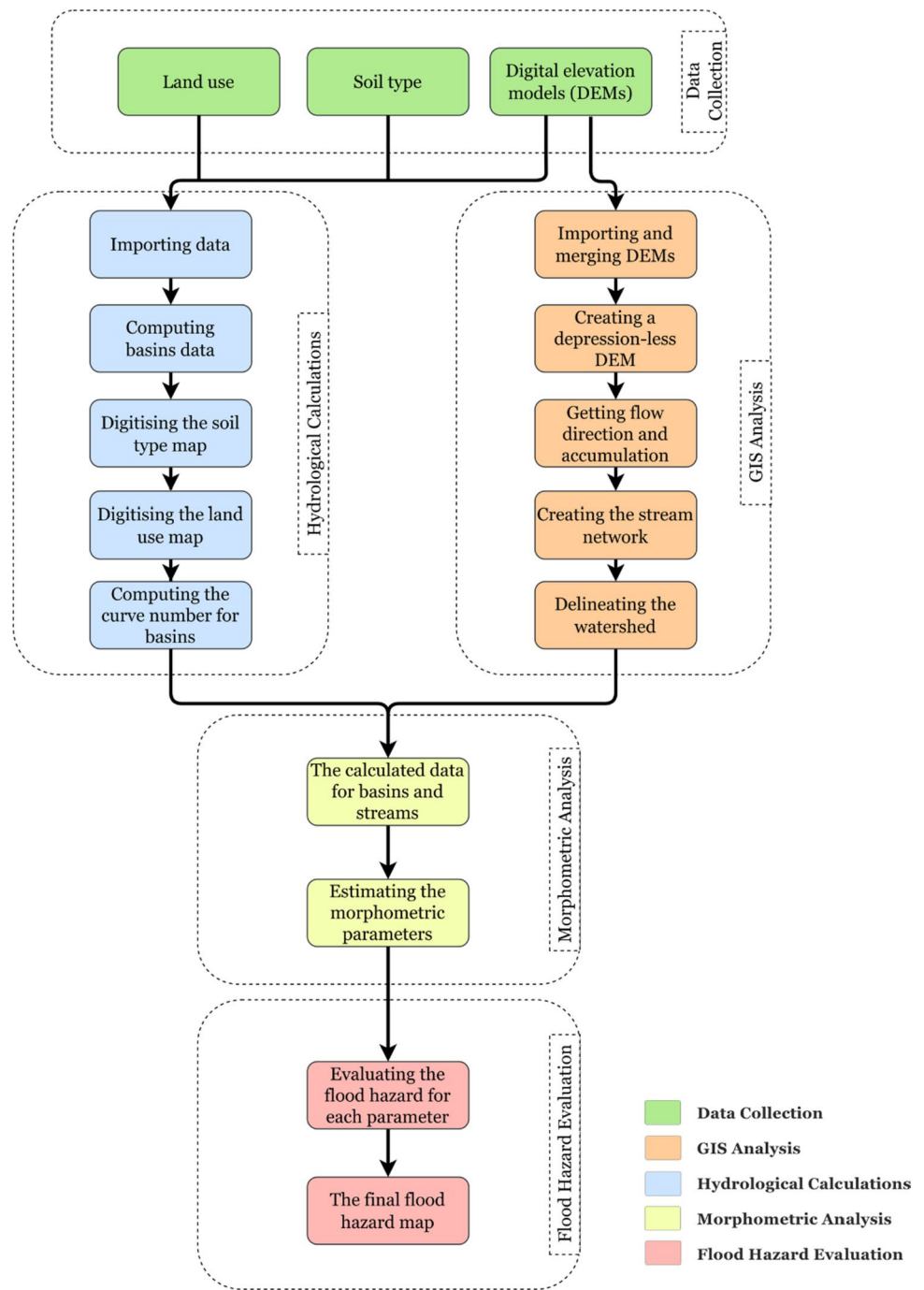
Materials and methods

The study employed GIS techniques and morphometric analysis to produce a flood hazard map for the study area. In doing so, land use and soil type maps, in addition to multiple digital elevation models (DEMs) with 30-m resolution that cover the study area, were first collected. Then, the DEMs were merged in a GIS environment, and multiple processes were carried out (e.g., correcting the DEM, generating the stream network and the delineation of the watershed). The land use and soil type maps were digitized in a hydrological environment to compute the curve number for the basins. After that, the morphometric parameters

of the basins in the study area were estimated, and the flood hazard degrees were calculated for each parameter. Finally, the overall flood hazard degrees were calculated, and the flood hazard map was produced. To validate morphometric-based flood hazards degree, the results are cross-compared with outcomes from a hydrological model, considering the hazards associated with peak discharges of the basins. Furthermore, the significance of the curve number in flood hazard assessment was tested by comparing results with and without its inclusion. The overall methodology followed in the study is illustrated in Fig. 3.

In this study, 13 DEMs are used. The DEMs are available from the US Geological Survey (USGS) Earth Explorer (US Geological Survey 2021). These elevation data provide global coverage of void-filled data with 1 arc-second (30 m) resolution and an open release of this high-resolution global dataset (US Geological Survey 2018). The soil type and land use data of the study area were obtained from the soil association map of Egypt (El-Ramady et al. 2019). The data show two different soil types in the study area: the first is “rugged rock land mainly of the basement complex,” and the second is “gravelly and gravelly sand beaches, sometimes with rock outcrops.” It also shows that there are two main classes of land use in the study area: “bare rock” and “bare soil very stony (deep soil).”

Fig. 3 Procedure for flood hazard mapping using GIS-morphometric estimation



Generation of the drainage network

The GIS analysis aimed to generate the stream network and delineate the watershed of the study area. The ArcGIS Pro software with version number 2.9.0 was used (ArcGIS Pro 2021). First, the coordinate system has been projected using the Egypt 1907/Red Belt coordinate system (EPSG 2014). Then, the 13 digital elevation models were merged into one DEM. A raster of flow direction from each cell to its downslope neighbor(s) was generated to remove the

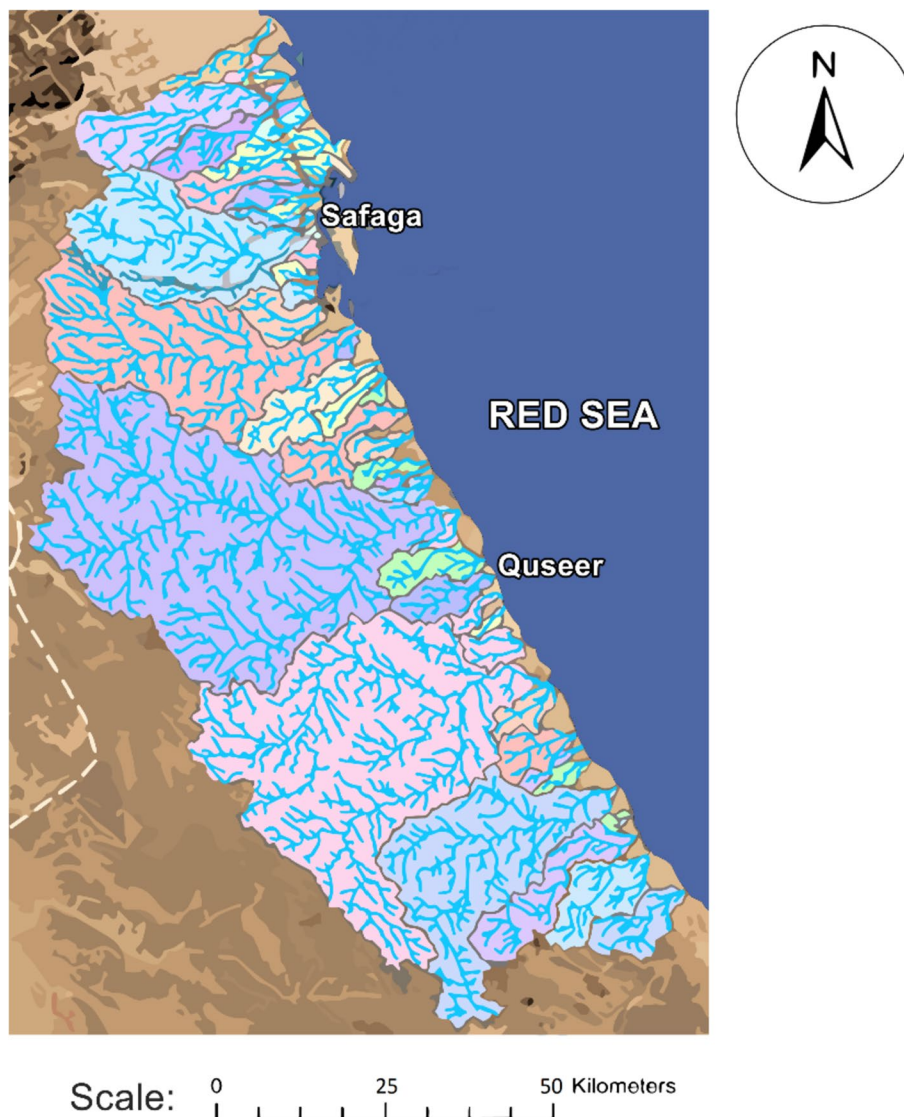
defects in the data. This method is known as an eight-direction (D8) flow model (Jenson and Domingue 1988). To produce a depression-less DEM, all sinks or areas of internal drainage were first detected, followed by statistical calculations, and then the sinks were filled using the fill tool in ArcGIS Pro, which uses the counterparts of multiple tools to fill all sinks. The tool can also be used to remove peaks, which are spurious cells with a higher height than would be predicted given the underlying surface trend.

A flow accumulation was then created to obtain the streams and, hence, extract the drainage network. The Strahler method was used to order streams (Strahler 1957). The Strahler method is the most commonly used approach for stream ordering. Stream order assigns numerical order to links in a stream network. This order is a method of recognizing and categorizing stream types depending on the number of tributaries. It is considered the major parameter in qualitative and quantitative analyses of any drainage basin (Elsadek et al. 2019a). Some stream characteristics can be deduced simply by knowing their order. The streams generated were then converted from the raster to features, and then the watershed delineation process was performed to preserve the drainage network of basins. The total drainage network containing basins and streams was clipped according to the boundary of the study area to derive the required drainage network. Finally, a joining process was done to join the streams and the basin into one drainage network

to act as a unit. From the previous analysis and watershed delineation, 43 basins have been identified. The watershed has a total area of 7,104.16 km², and the resulting drainage network has a total length of 5,154.68 km. Figure 4 shows the drainage network, including the generated basins from the GIS analysis.

An automated GIS model, which is called “Model Builder” in the ArcGIS Pro environment, has been developed to conduct the required processes for watershed delineation. The model successfully completed all the processes in only 39 min and 2 s. The PC used in the analysis has a processor with an Intel Core i7-10750H @ 2.60 GHz, 16 GB of RAM, and a 64-bit Windows 10 Home operating system. The automated GIS model significantly reduced the time and effort required to run the GIS processes on the digital elevation models (DEMs) used in the analysis. The automated model developed in this study has potential applications in other similar work that requires GIS analysis for morphometric

Fig. 4 Delineation of basins and drainage network generated through the GIS analysis



analysis. By automating the processes required for watershed delineation, this model can save time and effort when conducting GIS-based analysis. Future studies can benefit from using this model for similar work, particularly in large-scale study areas where processing multiple DEMs can be time-consuming and challenging.

Computation of the curve number for basins in a hydrological environment

The curve number is an empirical measure that is crucial in determining runoff in hydrological modeling (Ali et al. 2022). It was developed by the USDA Natural Resources Conservation Service, formerly known as the Soil Conservation Service, or SCS (Sherief 2008). To compute the curve number for the basins, the merged DEM was imported into a hydrological environment. The Watershed Modeling System (WMS) version 11.1.0, Aquaveo LLC (Aquaveo 2021), is employed here. Flow direction and accumulation processes were done for that DEM, followed by a conversion of the DEM to stream arcs to generate the streams. Then, the basin data were defined and computed. In order to obtain the curve number of each basin, both the soil type and land use data were digitized in the study area and defined. The land use of the developing urban areas, or newly graded areas, in the Red Sea Governorate was also considered and included in the digitizing process.

Estimation of the morphometric parameters for basins

In order to implement the morphometric analysis for the study area, various parameters were estimated based on the computed basin data from the previous steps. The considered morphometric parameters in this study depict a number of different features, including the drainage network aspect, which is represented by stream orders, stream lengths, stream number, stream frequency, and drainage density. In addition, they consider basin aspects, including areal characteristics such as basin area, dimensional characteristics such as basin length and perimeter, shape characteristics such as circularity ratio and shape factor, and surface characteristics reflected by basin slope. The curve number in this study represents the runoff aspect.

The area (A) of the basin is considered to be one of the most important elements in the morphometric analysis of stream systems (Sherief 2008). Strahler (1957) states that basins with similar characteristics in area and shape are also similar in their geomorphological characteristics. The basin slope (S) is the average basin slope, or average slope, of the cells comprising this basin. It is defined as the rate of rise or fall against horizontal distance; moreover, it is a measurement giving the steepness of the ground surface. The slope

gradient is a key factor affecting relative stability because it determines how strongly gravity acts on a soil mass (Sherief 2008). It is considered one of the main factors controlling surface flow and potential flooding (Helmi et al. 2019). The sinuosity index (SI), Schumm (1956) explains it as a factor to define a flow deviation from the expected straight path. It can be obtained by dividing the maximum stream length in the basin by the basin length, which is the length of the straight-line distance of the basin. The shape factor (SF) is the length of the basin divided by its width, or the ratio of the square of the basin length to the basin area (Eq. 1). The calculated shape factor in WMS is the inverse of the form factor, which is commonly used in similar studies and indicates the flow intensity of a basin in a defined area (Horton 1932). The smaller the form factor value (and therefore the larger the shape factor value), the more elongated the basin will be, while the higher values correspond to the basin being circular. The area, slope, sinuosity factor, and shape factor were all calculated in the WMS software.

$$SF = \frac{L_b^2}{A} \quad (1)$$

where L_b is the basin length in km, and A is the area of the basin in km^2 .

According to Miller (1953), the circularity ratio (CR) represents the relationship between the basin area and the area of a circle whose circumference is equal to the basin perimeter (Eq. 2). The values close to one are indicative of the greater circularity obtained by the basin, and vice versa. The circularity ratio for each basin was computed in Microsoft Excel software. Many factors influence the circularity ratio, including the length and frequency of the stream, land use, climate, land cover, geological composition, relief, and slopes of the basin (Elsadek et al. 2019a). Drainage intensity (DI) is defined as the ratio of stream frequency to drainage density (Eq. 3) (Faniran 1968). Drainage density represents channel closeness in the basin and can be defined as the ratio between the total stream lengths in the basin and the area of the basin. There are many factors affecting drainage density, such as relief, climatic changes, the type and permeability of rocks, and vegetation that controls the characteristic length of the stream (Moglen et al. 1998). Based on Horton (1945), stream frequency, which reflects the texture of the drainage network, is the ratio between the total number of stream segments of all orders in a basin and the basin area. For the curve number (CN), it was mentioned before that this parameter was computed in the hydrological environment using the WMS software based on the soil type and the land use.

$$CR = \frac{A}{A_c} = \frac{4\pi A}{P^2} \quad (2)$$

where A is the area of the basin in km^2 , A_c is the area of a circle with a circumference that equals the basin perimeter in km^2 , and P is the basin perimeter in km .

$$DI = \frac{F}{D_d} = \frac{N/A}{L_u/A} = \frac{N}{L_u} \quad (3)$$

where F is the stream frequency of the basin in km^{-2} , D_d is the drainage density of the basin in km^{-1} , N stands for the total number of streams of all orders, while L_u symbolizes the total stream lengths in the basin in km .

Evaluation of the flood hazard degrees for basins

For the considered parameters, a hazard scale was set and used to assess the flash flood hazard in the study area. This scale ranges between one and five. One means a very low degree of hazard, while two represents a low hazard degree. The third hazard degree points to a moderate level of hazard. The fourth and fifth hazard degrees for a basin indicate that the flood hazard degree for that basin is high and very high, respectively. The hazard degrees for the basins were calculated as follows:

- Find out the minimum and maximum values of each morphometric parameter for all basins.
- Calculate the actual hazard degree for all parameters using their minimum and maximum values. By assuming a linear relationship between degrees, the actual value of the hazard degree can be derived from the geometric relationship (Davis 1986).
- For parameters with a linear relationship:

$$\text{Hazard degree} = \frac{4 \times (Y - Y_{\min})}{(Y_{\max} - Y_{\min})} + 1 \quad (4)$$

- For parameters with an inverse linear relationship:

$$\text{Hazard degree} = \frac{4 \times (Y - Y_{\max})}{(Y_{\min} - Y_{\max})} + 1 \quad (5)$$

where Y is the value of the morphometric parameter for a basin, while Y_{\max} and Y_{\min} are the maximum and minimum values of the morphometric parameter for all basins, respectively. The evaluation Hazard degree per each parameter for all basins can be determined based on Eqs. 4 and 5.

- For each basin, the total hazard degree is calculated by summing up flood hazard degree for all parameters. Subsequently, these values are used to estimate the overall hazard degree per each basin using Eq. 4, resulting in values ranging from one to five.

Results and discussion

Morphometric analysis of the drainage basins

The study area contains 43 basins, with basin areas ranging from 6.55 km^2 to $1,797.69 \text{ km}^2$. The average area of the basins is 165.21 km^2 , while the average perimeter of the basins is about 80.19 km . The watershed has a total of 2,523 streams, linked in a fiveorder of stream network. The number of streams inversely proportional to the stream order, with the largest number of streams in first-order (1287 streams). The minimum basin length was found to be 5.40 km for basin B17, while the maximum is 67.46 km for basin B33 (see Fig. 5). The average slope of the basins is 0.14 , while the average sinuosity index of the basins was found to be 1.23 . The circularity ratio for the basins ranges from 0.12 to 0.31 . The minimum curve number is 72.26 , while the maximum value was found to be 94 . The drainage density for the basin in the study area ranges from 0.49 to 2.35 km^{-1} , while the values of stream frequency ranges from 0.19 to 0.76 km^{-2} . The low values of stream frequency indicates a scarce plant cover (Elsadek et al. 2019a). The values of drainage intensity for the basins are in the range of 0.27 – 0.58 km^{-1} . The high values of the drainage intensity for the basins indicate a soil erosion susceptibility (Elsadek et al. 2019a). The values of the shape factor for the basins are in the range of 2.08 to 10.15 . The morphometric parameters considered in the flood hazard assessment are shown in Table 1.

Flood hazard assessment

The final flood hazard map for the study area is shown in Fig. 5, and the overall hazard degrees for the basin are in Table 2. There are four basins with a very low hazard degree and 11 basins with a low hazard degree. It was also found that 16 basins have a medium hazard degree. On the other hand, the results show that 12 basins have high or very high hazard degrees. These basins cover an area of about $5,717.51 \text{ km}^2$ representing about 80% of the total study area. The basins with the highest hazard degree are basins B33 and B42, whose areas are $1,797.69 \text{ km}^2$ and $1,530.65 \text{ km}^2$, respectively. These two basins cover about 47% of the study area. The low flood vulnerability of the basins with low or very low hazard degrees can be explained by their morphometric parameters. The most common feature among these basins is the high value of the shape factor, ranging from 3.22 (B17) to 10.15 (B12). The basins are also characterized by small slopes, ranging from 4.25 (B2) to 25.07% (B10), small areas, ranging from 6.55 km^2 (B2) to 224.14 km^2 (B5), and small circularity ratios, ranging from 0.12 (B36) to 0.3 (B17). The low values of slope, area, and circularity ratio, as

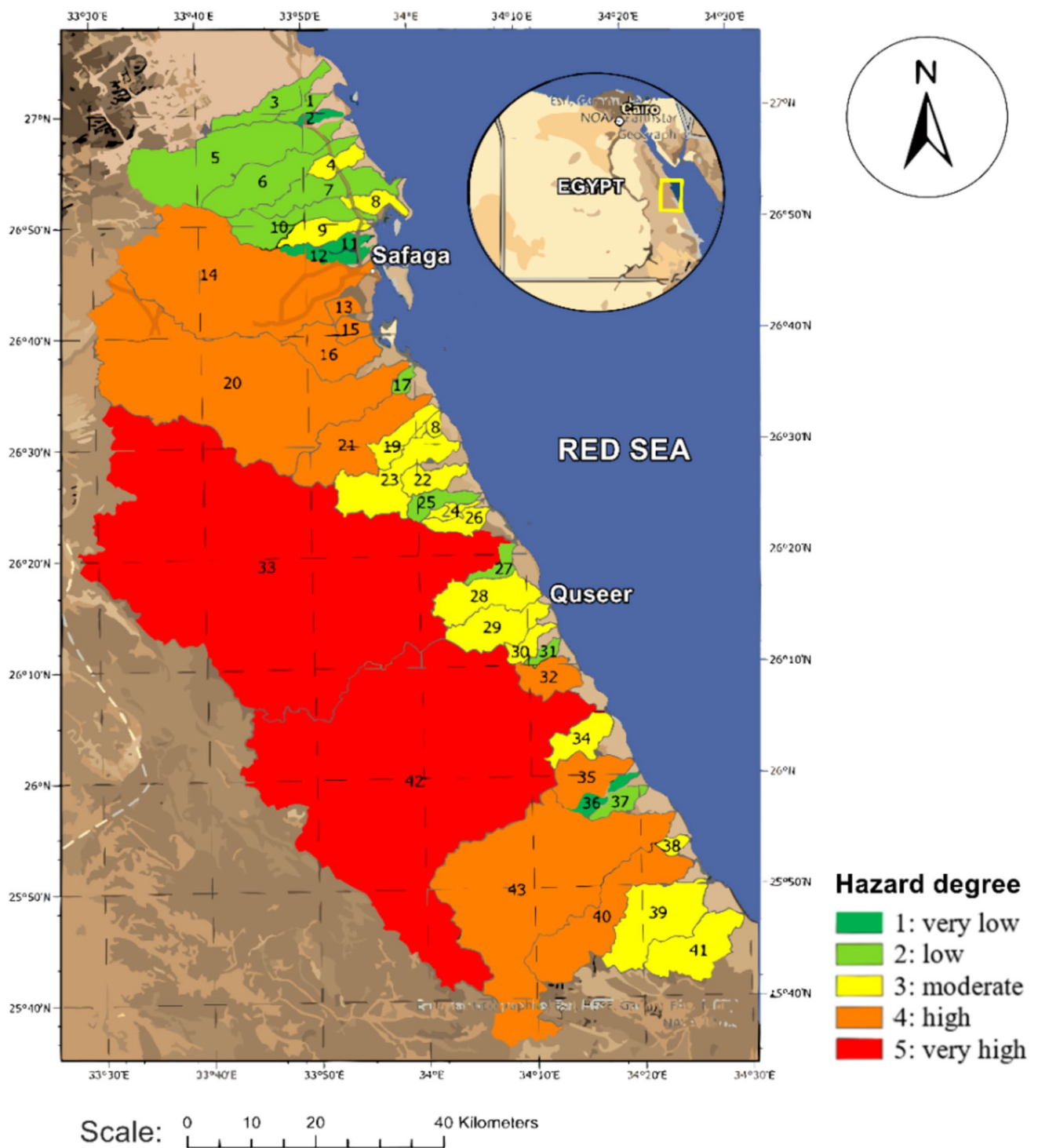


Fig. 5 Flood hazard map of the study area

well as the high value of the shape factor, suggest their low vulnerability to flooding (Obeidat et al. 2021; Elsadek et al. 2019a; Redwan et al. 2021).

Similarly, the geomorphometric characteristics can help illustrate the high hazard degree in the basins. These basins

have low values of the shape factor, ranging from 2.08 (B32) to 5.29 (B40) and steep slopes, ranging from 10.92 (B35) to 36.16% (B15), which accordingly result in high flow velocities, low infiltration, and higher flood peaks (Ogarekpe et al. 2020). Moreover, the curve number for these basins is high,

Table 1 Morphometric parameters of the basins

Basin no	Area (km ²)	Slope (%)	Sinuosity index	Shape factor	Curve number	Drainage intensity (km ⁻¹)	Circularity ratio
B1	14.57	4.90	0.93	6.92	77.00	0.41	0.17
B2	6.55	4.25	0.85	9.41	77.00	0.57	0.13
B3	36.78	4.75	1.31	5.52	77.00	0.44	0.17
B4	25.03	4.77	1.00	3.88	79.72	0.56	0.28
B5	224.14	19.63	1.31	5.48	72.26	0.39	0.16
B6	109.15	19.32	1.34	6.62	76.04	0.35	0.16
B7	73.77	9.39	1.25	6.15	82.10	0.39	0.15
B8	8.42	4.00	1.09	5.14	94.00	0.33	0.21
B9	51.35	12.88	1.09	4.54	80.80	0.37	0.24
B10	75.87	25.07	1.15	7.35	85.31	0.41	0.13
B11	7.17	4.32	0.92	9.90	86.71	0.30	0.13
B12	18.75	17.84	1.14	10.15	75.05	0.30	0.12
B13	15.19	33.24	0.98	3.49	92.50	0.46	0.24
B14	506.09	23.71	1.43	3.21	86.66	0.53	0.21
B15	7.90	36.16	0.93	3.95	94.00	0.42	0.31
B16	49.56	22.8	1.32	3.69	89.09	0.43	0.22
B17	9.04	6.61	0.93	3.22	77.00	0.36	0.30
B18	10.76	9.14	1.10	3.57	77.00	0.43	0.25
B19	37.49	15.00	1.28	5.11	86.03	0.61	0.18
B20	719.00	18.70	1.59	3.42	88.04	0.50	0.16
B21	142.17	19.06	1.33	4.74	87.48	0.50	0.14
B22	31.51	14.35	1.23	3.70	87.66	0.44	0.23
B23	108.76	18.69	1.39	4.44	86.52	0.50	0.13
B24	26.57	12.16	1.15	4.62	90.36	0.39	0.21
B25	26.31	14.17	1.14	5.37	86.20	0.39	0.16
B26	26.96	12.37	1.20	4.47	88.78	0.33	0.19
B27	12.87	12.34	1.17	6.96	81.64	0.33	0.14
B28	57.13	11.73	1.30	5.11	84.48	0.54	0.13
B29	79.64	15.07	1.23	3.59	85.83	0.52	0.22
B30	23.85	14.08	1.44	4.54	82.10	0.53	0.16
B31	10.38	14.85	1.15	4.59	77.00	0.35	0.21
B32	46.87	14.21	1.21	2.08	77.55	0.48	0.31
B33	1797.69	19.84	1.49	2.53	88.06	0.49	0.17
B34	34.64	13.33	1.22	4.40	83.59	0.37	0.16
B35	66.71	10.92	1.27	2.77	83.06	0.40	0.26
B36	19.79	8.48	1.12	7.43	85.18	0.27	0.12
B37	20.11	8.74	1.19	5.62	80.35	0.52	0.16
B38	8.93	7.09	0.99	3.30	77.00	0.48	0.30
B39	98.09	11.38	1.37	4.55	87.90	0.50	0.18
B40	184.86	18.38	1.54	5.29	87.79	0.58	0.12
B41	92.27	8.62	1.37	3.29	87.12	0.42	0.22
B42	1530.65	17.34	1.76	2.11	84.67	0.51	0.15
B43	650.82	18.05	1.65	3.35	87.44	0.55	0.14

ranging from 77.55 (B32) to 94 (B15), which increases the runoff and hence the flood vulnerability (Khalil 2018). The basins with the highest hazard degree (very high) are basins B33 and B42. This is because of the large area of

the basins, which has a direct impact on flood vulnerability (Obeidat et al. 2021; Elsadek et al. 2019a). In addition, the shape factors for the two basins are low: 2.53 (B33) and 2.11 (B42), indicating high peak flows with shorter durations and

Table 2 Hazard degrees for the basins

Basin no	Hazard degree*
B33 and B42	5
B13, B14, B15, B16, B20, B21, B32, B35, B40, and B43	4
B4, B8, B9, B18, B19, B22, B23, B24, B26, B28, B29, B30, B34, B38, B39, and B41	3
B1, B3, B5, B6, B7, B10, B17, B25, B27, B31, and B37	2
B2, B11, B12, and B36	1

* 5: very high, 4: high, 3: moderate, 2: low, and 1: very low

resulting in high flood vulnerability (Elsadek et al. 2019a; Joji et al. 2013; Adhikari 2020; Obeidat et al. 2021). Furthermore, the two basins have high numbers of first-order streams, suggesting their high potential for flooding (Ogarkpe et al. 2020).

The impact of parameters on hazard degree is represented in the correlation matrix, as shown in Fig. 6. This study uses the Python programming language to calculate correlation coefficients between the morphometric parameters and hazard degree and the Seaborn data visualization library to visualize the results (Seaborn 2022). The matrix was obtained using the most common Pearson product-moment correlation coefficient formula (Eq. 6) (Moore et al. 2013). As shown in the bottom row of the matrix, the shape factor has the most significant impact on the hazard degree, with a high negative value (−0.82). Area and sinuosity factor has the same positive correlation coefficient of 0.57, followed by curve number, drainage density, and slope with positive coefficients of 0.51, 0.5, and 0.48, respectively. Finally, the circularity ratio has a value of 0.33. These results are consistent with the findings from the literature discussed above

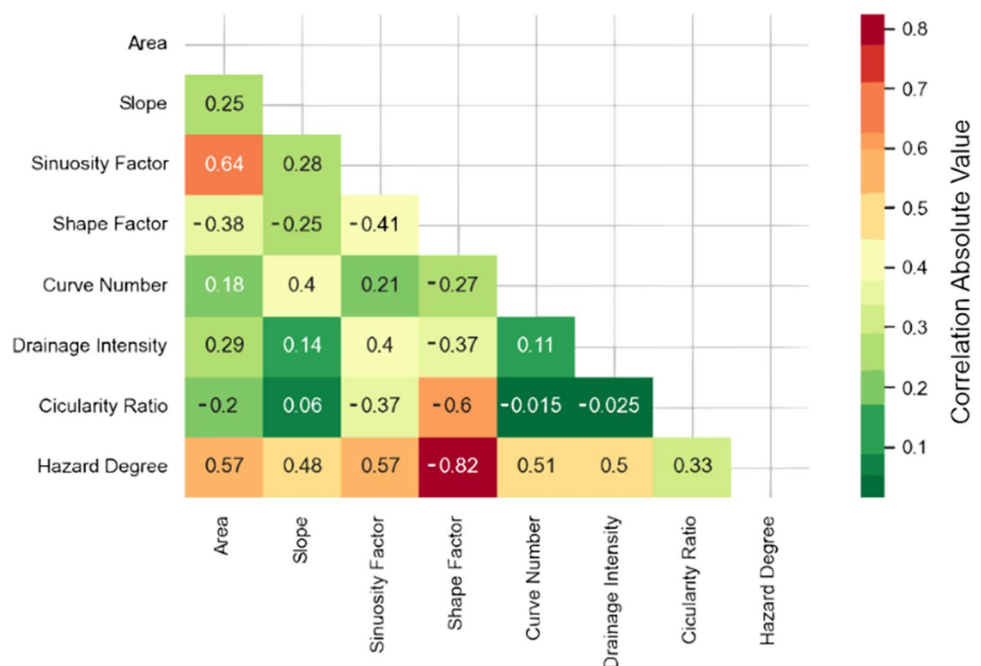
on the impact of the morphometric parameters used in this study on flood vulnerability.

$$r_{xy} = \frac{\sum_{i=1}^n (x_i - \bar{x})(y_i - \bar{y})}{\sqrt{\sum_{i=1}^n (x_i - \bar{x})^2 \sum_{i=1}^n (y_i - \bar{y})^2}} \tag{6}$$

where (r_{xy}) is the correlation coefficient between two variables X and Y , n is the number of dataset instances (here is the number of basins), x_i and y_i are the data points for the two variables for each instance, and \bar{x} and \bar{y} are the means of the x and y values, respectively.

This study shows that basin B33, which is known as Wadi Queih, and basin B42, which is known as Wadi El-Ambagi, in the western section of the study area have very high hazard degrees. Our results are consistent with previous findings in the literature. For example, Nasr et al. (2022) used statistical and geospatial approaches, in addition to remote sensing data, to identify potential flash flood hazard areas in Wadi Queih and found that there is a significant risk of flooding in that area. Mashaly and Ghoneim (2018) studied

Fig. 6 Correlation matrix for morphometric parameters and hazard degree



the characteristics of surface runoff in Wadi El-Ambagi, which is home to one of the few road networks connecting the Nile River Valley to the Red Sea coast. The study used a hydrological modeling approach in addition to a hydraulic model and found that a flood of 60 mm would surge certain areas of Quseir with flood waters up to 2 m deep, inundating hundreds of buildings, segments of the Qift-Quseir highway, and the phosphate railroad. Monsef (2018), who used a hydrological model, and Zaid (2009), who carried out hillslope analysis, also reported that Wadi El-Ambagi is a flood-prone area. Youssef et al. (2009) used geological and geomorphological properties in a GIS-based environment to create hazard maps that identify Wadi El-Ambagi as one of the Red Sea coast's flood-prone regions. There were two types of failures recorded in the study along the roads in that area due to flash floods. As expressed, the results of the current study and previous studies are consistent, as they all confirm that the two basins, Wadi Queih and Wadi El-Ambagi, are identified as severe flood-prone areas across different approaches and methodologies. This agreement confirms the validity of GIS-based morphometric analysis approach used in this study and its potential in flood risk analysis.

The outcomes of the morphometric analysis for flood hazard mapping in the study area are compared to the outputs of a hydrological model. The Hydrologic Modeling System (HEC-HMS) software, version 4.4.1 (US Army Corps of Engineers Hydrologic Engineering Center 2020), is employed here. Available rainfall data for the study area was obtained from the global weather data for SWAT (Soil Water Assessment Tool 2014) over a 36-year period from 1979 to 2014. Rainfall records and their temporal distribution in the sub-basins were defined, and then the basin model was created in HEC-HMS. After that, a rainfall simulation with a precipitation rate of 50 mm/year was employed. The value of the precipitation was chosen to be uniform for the whole area to harmonize the spatial difference in rainfall in the study area. This value is the average of daily precipitation of the most severe rainfall events that occurred across the whole study area, estimated at 50 mm/year. The peak discharge and runoff depth (volume per basin area) of the basins are shown in Table 3. Peak discharges were then classified into ranks from one to five in ArcGIS Pro with the same calculation procedure as hazard degrees, and a peak rank map was produced as shown in Fig. 7.

Overall, the hydrological model and its runoff peak ranks show similar hazard degrees that result from the GIS model (see Fig. 8). The outcomes of the model show that the basins B33 and B42, which have very high hazard degrees, have the highest peak ranks with discharges of 700 and 485.5 m³/s, respectively. The volumes of rainfall in these two basins are 42.04 and 28.74 Mm³, which are also the highest among all basins. It was also found that the basins having high or very high peak ranks are: B14, B20, B33, B42, and B43, which

Table 3 Output peak discharge and runoff depth values for the basins

Basin no	Peak discharge (m ³ /s)	Runoff depth (mm)	Basin no	Peak discharge (m ³ /s)	Runoff depth (mm)
B1	8.30	10.96	B23	83.00	21.69
B2	4.10	10.96	B24	44.90	27.73
B3	15.30	10.96	B25	34.60	21.24
B4	19.20	13.52	B26	43.70	25.10
B5	41.40	7.27	B27	11.90	15.55
B6	33.20	10.13	B28	40.60	18.94
B7	49.70	16.07	B29	75.80	20.73
B8	21.70	34.72	B30	20.60	16.07
B9	40.20	14.64	B31	7.10	10.96
B10	61.20	20.02	B32	27.20	11.45
B11	11.80	21.96	B33	700.00	23.39
B12	8.20	9.33	B34	30.20	17.82
B13	41.70	31.67	B35	52.10	17.18
B14	270.30	21.88	B36	20.20	19.85
B15	30.10	34.72	B37	15.80	14.16
B16	66.40	25.59	B38	7.10	10.96
B17	6.90	10.96	B39	93.70	23.72
B18	7.70	10.96	B40	132.20	23.55
B19	36.80	21.00	B41	84.00	22.56
B20	335.80	23.78	B42	485.50	18.78
B21	105.70	23.09	B43	301.70	22.92
B22	42.40	23.36			

are all marked as high or very high in hazard degrees. Moreover, the two models show an agreement on all the basins with low flood vulnerability (basins B1, B2, B3, B5, B6, B7, B10, B11, B12, B17, B25, B27, B31, B36, and B37). Such results show agreement between the two models, indicating that the study's GIS-based morphometric analysis approach can be applied for future research to identify highly vulnerable areas to flooding. To further evaluate the curve number's significance in flood risk assessment, we compare the flood hazards with and without considering the curve number. The results, as shown in Fig. 9, indicate that omitting the curve number in the morphometric analysis overestimates the flood hazard degree in one-third of the basins. This suggests that incorporating the curve number, a representative of runoff, in flood hazard assessment enhances the accuracy of estimating flood risk (Ali et al. 2022; Lee et al. 2023).

The study area is an arid region primarily covered with bare vegetation. Although the area experiences intense rainfall intermittently throughout the year, it is also subject to drought due to lack of rainfall throughout the year. While heavy rainfall leads to flooding, prolonged droughts amplify soil susceptibility to erosion and nutrient deficiency (Olsson et al. 2019). Understanding watershed

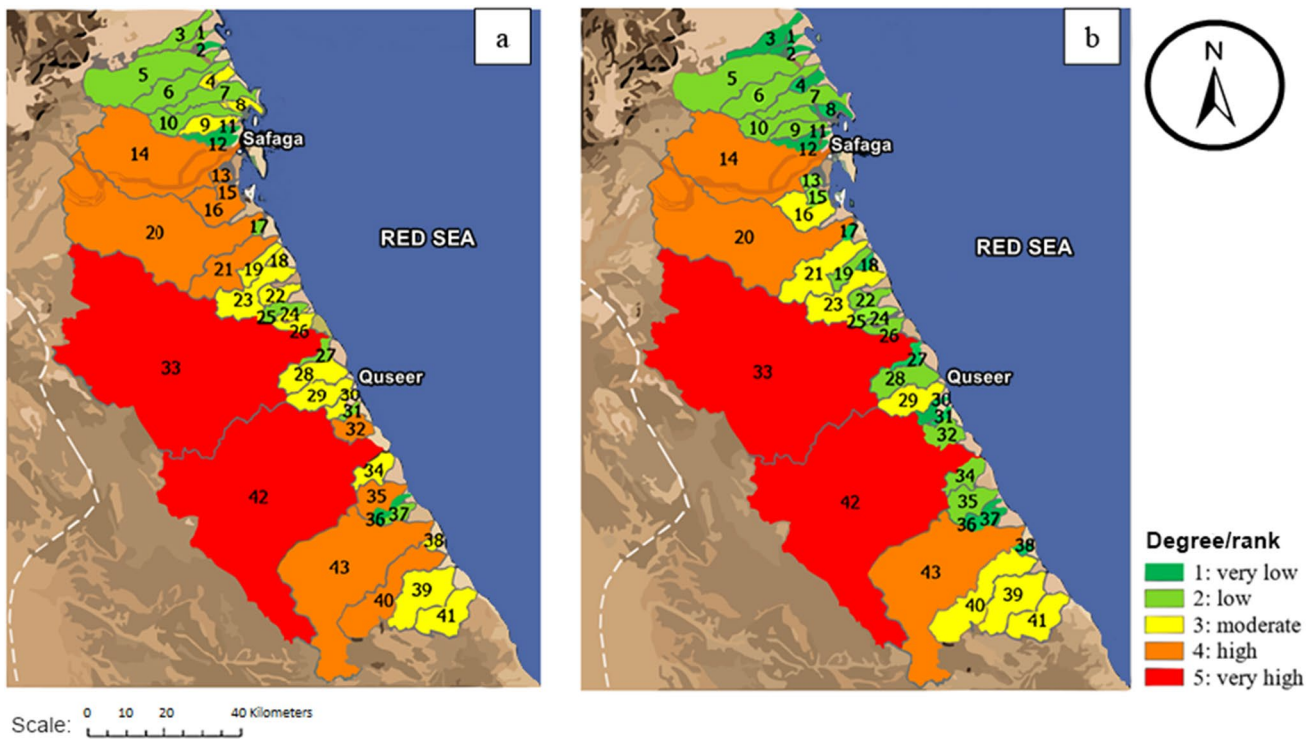


Fig. 7 a Flood hazard degree map (left) vs b Peak runoff rank map (right)

hydrology is pivotal for prioritizing conservation efforts, mitigating drought impacts, and improving watershed management (Abdeta et al. 2020). Morphometric analysis plays a significant role in this context, with parameters like stream frequency and drainage density directly influencing drought conditions and soil erodibility (Elsadek et al. 2019a; Tesema 2021). Basins exhibiting high values in these parameters, such as B2, B8, B11, and B15, indicate a greater vulnerability to drought susceptibility. Furthermore, factors like concentration time, driven by shape factor and circularity ratio parameters (Potter and Faulkner 1987; Bali et al. 2012), play an important role in triggering a drought. Basins with high shape factor values tend to have longer concentration times, while those with high circularity ratios have shorter concentration times. Therefore, basins with high circularity ratio and small shape factors such as B4, B13, B17, B20, B22, B29, B35, and B41 are prone to drought risk. Furthermore, the slope of a basin is also a critical factor influencing drought and soil erosion (Masroor et al. 2022). Basin with high slopes such as B13 and B15 are particularly susceptible to drought. These results highlight the role of geomorphological parameters in analyzing drought susceptibility. Furthermore, they underscore the necessity for robust conservation measures in drought-prone basins and proactive water management strategies to alleviate drought impacts.

Recommendations to achieve sustainable development goals (SDGs)

Egypt’s commitment to achieving sustainable development goals is evident by the launch of Egypt Vision 2030, and the signature of the Strategic Framework for Partnership with the United Nations (UN) (Egypt State Information Service (SIS) 2023). Understanding basin geometry and drainage network parameters is crucial for minimizing economic impacts from floods. Unmanaged flash floods can damage railways, highways, like those between Safaga and Quseir, harbors, like the Safaga harbor, and other infrastructure, especially in regions with high slopes. Land topography and past rainfall information should be considered to avoid economic losses caused by flash floods. The study area, as shown, is vulnerable to flash floods that are expected to increase in the future due to climate change (Zhang et al. 2021). Therefore, identifying flood-prone areas using flood hazard mapping can protect local communities and contribute to achieving the SDGs and their targets. The SDGs encourage reducing and adapting to their effects. This study directly addressed Target 1.5, “Reduce climate-related extreme events.”, Target 11.2, “Provide safe and sustainable transport systems and improve road safety”. The flood map produced here can be used by the disaster management team to identify flood-prone areas, prioritize response efforts, and prepare emergency measures. Although basins B33 (Wadi Quier) and B42 (Wadi El-Ambagi) have very high hazard degrees,

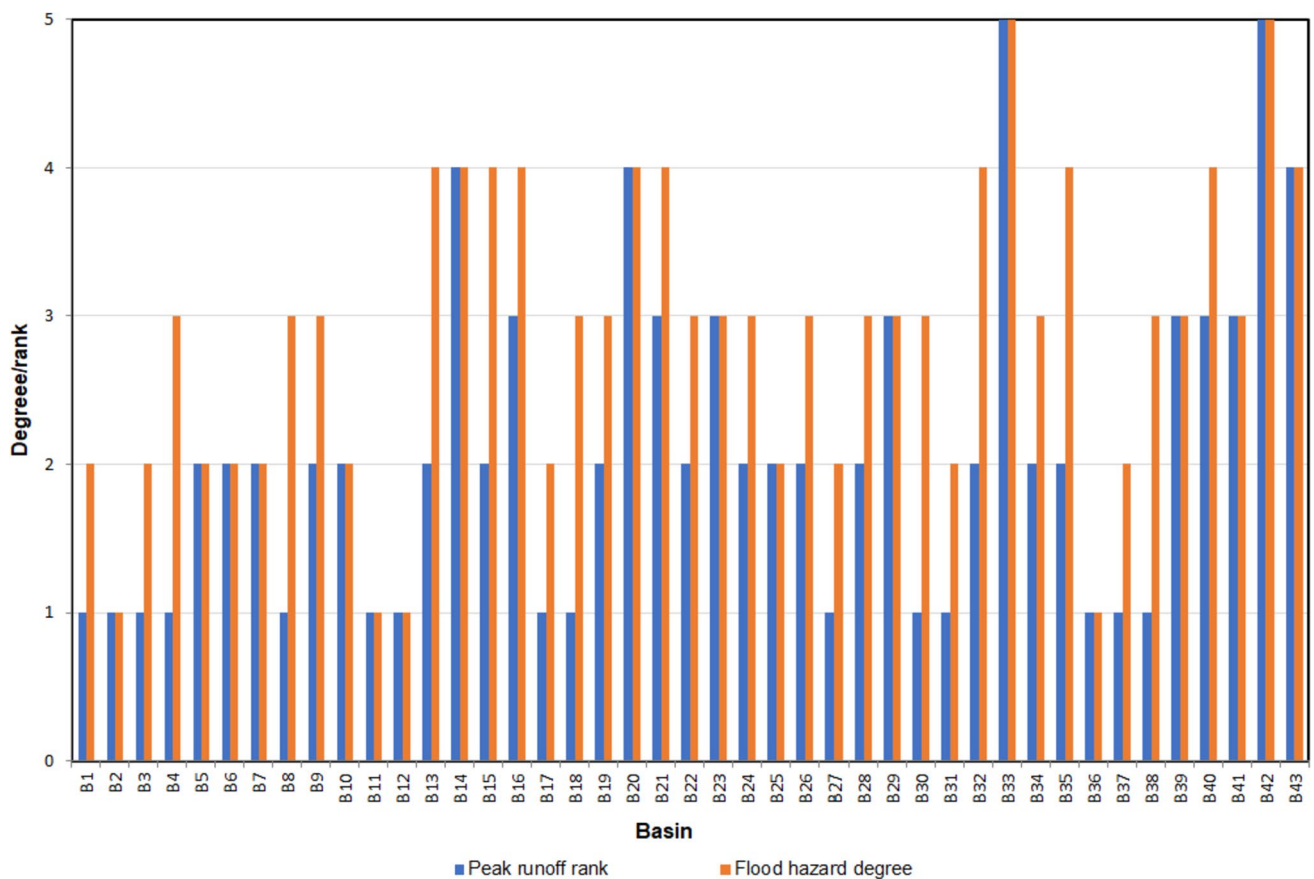


Fig. 8 Comparison of flood hazard degrees based on morphometric parameters and peak runoff ranks

they could have high water volumes. Thus highlighting their potential contribution to improving water supply management in the region. For example, water harvesting facilities and small dams can be constructed in these basins to harvest storm water, mitigate flood risks, and recharge groundwater aquifers. Accordingly, the following targets can be achieved: Target 6.5, “Implement integrated water resources management,” and Target 12.2, “Sustainable management of natural resources.” On the other hand, future studies could benefit from the engagement of local communities and stakeholders in effective flood risk management. This can help achieve Targets 6.b, “Participation of local communities in water management,” and 12.8, “Promote awareness for sustainable development.” Overall, the linkage between flood hazard mapping and the SDGs can help reduce the detrimental consequences of flash floods and promote sustainable development.

Conclusion

This study presents a GIS-based morphometric analysis framework to analyze flood risk. The developed framework was applied to a case study located between the Safaga and

Quseir regions along the Red Sea coast in Egypt. This logistic region is critical to the tourism industry and is vulnerable to frequent flash floods. The approach considers various morphometric parameters, representing geomorphological characteristics of the catchment such as basin area, slope, sinuosity factor, shape factor, drainage intensity, circularity ratio, and curve number. The watershed and drainage network were delineated using the ArcGIS Pro environment, where 43 subbasins were identified in the study area. An automated GIS model has been developed to expedite GIS processes reaching the delineation stage. This can be useful for large-scale studies by efficiently handling multiple DEMs, which can be time-consuming and challenging. Following the delineation process, the morphometric parameters were estimated and used to calculate the hazard degree per basin. The hazard degree was identified according to a five-grade scale ranging from very low to very high. The resulted flood hazard map can be used to determine vulnerable areas to flood risk. Results showed that there are two basins subjected to a very high hazard degree and ten basins with a high hazard degree. The 12 basins cover about 80% of the study area, suggesting the high vulnerability of the study area to floods.

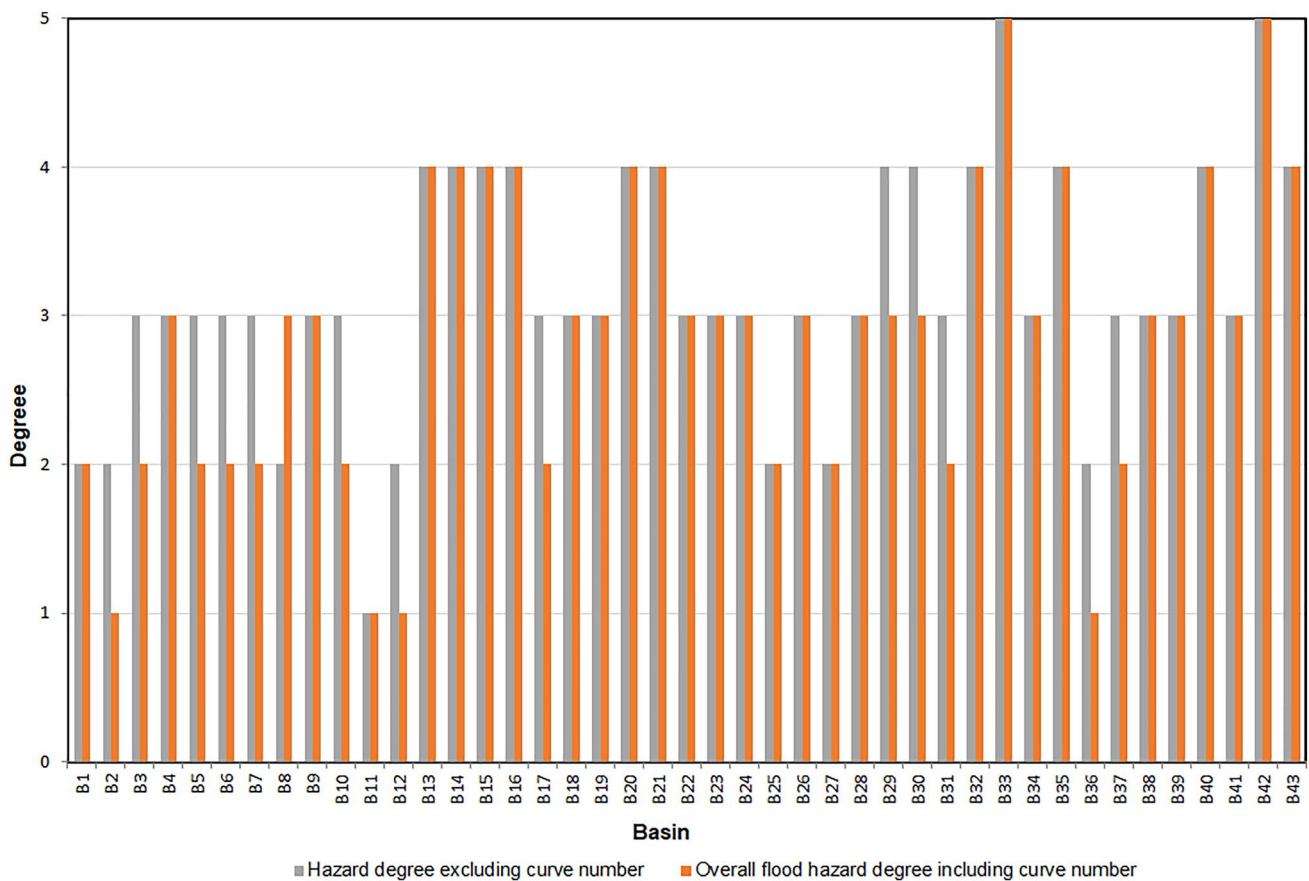


Fig. 9 Overall flood hazard degrees with and without curve number

The results of the morphometric analysis were compared to the hydrological simulation carried out using the HEC-HMS model. High runoff values were observed in the basins with high to very high hazard degrees, and vice versa. For example, specifically, the two basins with a very high hazard degree were also found to have the highest peak discharges of (B33) 700 and (B42) 486 m³/s. This suggests that the morphometric analysis aligns with the hydrological characteristics of the basin and their role in flood risk analysis. This also further justifies the results of the morphometric analysis presented here. On the other hand, the inclusion of the curve number in morphometric analysis enhances the flood risk assessment. The results presented above suggest that the study area is highly vulnerable to flash floods. This vulnerability could further increase in the future due to climate change. Therefore, identifying flood-prone areas using morphometric analysis, like in this study, can help protect local communities and reduce economic losses. Finally, the results of this study contribute to achieving SDGs through providing insights from flood hazard analysis. These insights can inform policy and decision-making processes aimed at reducing flood risks and promoting sustainable development.

Funding The corresponding author acknowledges the Faculty of Geosciences at Utrecht University, The Netherlands for supporting the publication fees for this article through the Geo Open Access fund.

Declarations

Conflict of interest The authors have no competing interests to declare.

Open Access This article is licensed under a Creative Commons Attribution 4.0 International License, which permits use, sharing, adaptation, distribution and reproduction in any medium or format, as long as you give appropriate credit to the original author(s) and the source, provide a link to the Creative Commons licence, and indicate if changes were made. The images or other third party material in this article are included in the article's Creative Commons licence, unless indicated otherwise in a credit line to the material. If material is not included in the article's Creative Commons licence and your intended use is not permitted by statutory regulation or exceeds the permitted use, you will need to obtain permission directly from the copyright holder. To view a copy of this licence, visit <http://creativecommons.org/licenses/by/4.0/>.

References

Abdeta GC, Tesemma AB, Tura AL, Atlabachew GH (2020) Morphometric analysis for prioritizing sub-watersheds and management planning and practices in Gidabo Basin, Southern Rift Valley

- of Ethiopia. *Appl Water Sci* 10:158. <https://doi.org/10.1007/s13201-020-01239-7>
- Abuzeid TS, Ashour MA, Mahmoud H (2022) Documenting and analyzing the harmful impacts of the seasonal floods in upper Egypt on Qena-Safaga railway track infrastructure. *JES J Eng Sci* 1:1–10. <https://doi.org/10.21608/jesaun.2022.140354.1139>
- Adhikari S (2020) Morphometric analysis of a drainage basin: a study of Ghatganga river, Bajhang district. *Nepal Geograph Base* 7:127–114. <https://doi.org/10.3126/tgb.v7i0.34280>
- Ali MH, Orabi AA, Alkhashab MH, Sleem E-MM (2022) Flood hazard assessment using geographic information systems of Wadi El-Dukhan, western desert, Sohag Governorate Egypt. *J Egypt Acad Soc Environ Develop* 23:51–70. <https://doi.org/10.21608/JADES.2022.247632>
- Almasalmeh O, Eizeldin M (2020) Flash flood modelling of ungagged watershed based on geomorphology and kinematic wave: case study of Billi drainage basin Egypt. *Int Water Technol J* 10:193–205
- Al-Qudah K (2011) Floods as water resource and as a hazard in arid regions: a case study in southern Jordan. *Jordan J Civ Eng* 5:148
- Amaechina EC, Anugwa IQ, Agwu AE et al (2022) Assessing climate change-related losses and damages and adaptation constraints to address them: evidence from flood-prone riverine communities in Southern Nigeria. *Environ Dev* 44:100780. <https://doi.org/10.1016/j.envdev.2022.100780>
- Aquaveo (2021) WMS-the all-in-one watershed Solution. <https://www.aquaveo.com/software/wms-watershed-modeling-system-introduction>. Accessed 7 Mar 2023
- Arnous MO, El-Rayes AE, El-Nady H, Helmy AM (2022) Flash flooding hazard assessment, modeling, and management in the coastal zone of Ras Ghareb City, Gulf of Suez Egypt. *J Coast Conserv* 26:0916. <https://doi.org/10.1007/s11852-022-00916-w>
- Bali R, Agarwal KK, Nawaz Ali S et al (2012) Drainage morphometry of Himalayan Glacio-fluvial basin, India: hydrologic and neotectonic implications. *Environ Earth Sci* 66:1163–1174. <https://doi.org/10.1007/s12665-011-1324-1>
- Bogale A (2021) Morphometric analysis of a drainage basin using geographical information system in Gilgel Abay watershed, Lake Tana Basin, upper blue Nile basin Ethiopia. *Appl Water Sci* 11:01447. <https://doi.org/10.1007/s13201-021-01447-9>
- Cappelli F, Tauro F, Apollonio C et al (2023) Feature importance measures to dissect the role of sub-basins in shaping the catchment hydrological response: a proof of concept. *Stoch Env Res Risk Assess* 37:1247–1264. <https://doi.org/10.1007/s00477-022-02332-w>
- Central Agency for Public Mobilization and Statistics (2015) The annual report to the statistics of the environment. https://www.capmas.gov.eg/Pages/Publications.aspx?page_id=5104&YearID=23371. Accessed 3 Nov 2023
- Davis JC (1986) *Statistics and data analysis in geology*, 2nd edn. Wiley
- Diakakis M (2011) A method for flood hazard mapping based on basin morphometry: application in two catchments in Greece. *Nat Hazards* 56:803–814. <https://doi.org/10.1007/s11069-010-9592-8>
- Egypt State Information Service (SIS) (2023) Egypt-United Nations partnership for sustainable development cooperation. <https://www.sis.gov.eg/Story/181591/Egypt-United-Nations-Partnership-for-Sustainable-Development-Cooperation>. Accessed 19 Aug 2023
- Egypt Today staff (2020) Video: 7 Upper Egypt-Red Sea highways closed after rains, flood falling from mountain swamps western Luxor. In: *Egypttoday*. <https://www.egypttoday.com/Article/1/91671/Video-7-Upper-Egypt-Red-Sea-highways-closed-after-rains>. Accessed 30 Oct 2023
- El MHA (2018) A mitigation strategy for reducing flood risk to highways in arid regions: a case study of the El-Quseir–Qena highway in Egypt. *J Flood Risk Manag* 11:S158–S172. <https://doi.org/10.1111/jfr3.12190>
- Elnazer AA, Salman SA, Asmoay AS (2017) Flash flood hazard affected Ras Gharib city, Red Sea, Egypt: a proposed flash flood channel. *Nat Hazards* 89:1389–1400. <https://doi.org/10.1007/s11069-017-3030-0>
- El-Ramady H, Alshaal T, Bakr N et al (2019) *The soils of Egypt*, 1st edn. Springer
- Elsadek WM, Ibrahim MG, Mahmud WE (2019a) Runoff hazard analysis of Wadi Qena Watershed, Egypt based on GIS and remote sensing approach. *Alex Eng J* 58:377–385. <https://doi.org/10.1016/j.aej.2019.02.001>
- Elsadek WM, Ibrahim MG, Mahmud WE, Kanae S (2019b) Developing an overall assessment map for flood hazard on large area watershed using multi-method approach: case study of Wadi Qena watershed. *Egypt Natl Hazards* 95:739–767. <https://doi.org/10.1007/s11069-018-3517-3>
- Elsayad MAM (2013) Risk assessment of flash flood in Sinai. College of Engineering and Technology, Arab Academy for Science, Technology & Maritime Transport
- EPSG (2014) Egypt 1907 / Red Belt - EPSG:22992. <https://epsg.io/22992>. Accessed 30 Sep 2022
- Faniran A (1968) The index of drainage intensity a provisional new drainage factor. *Aust J Sci* 31:328–330
- Gabr ME, El-Ghandour HA, Elabd SM (2023) Prospective of the utilization of rainfall in coastal regions in the context of climatic changes: case study of Egypt. *Appl Water Sci* 13:18359. <https://doi.org/10.1007/s13201-022-01835-9>
- Hagos YG, Andualem TG, Yibeltal M, Mengie MA (2022) Flood hazard assessment and mapping using GIS integrated with multi-criteria decision analysis in upper Awash River basin Ethiopia. *Appl Water Sci* 12:01674. <https://doi.org/10.1007/s13201-022-01674-8>
- Harris County Flood Control District (2023) Interactive mapping tools. <https://www.hcfd.org/Resources/Interactive-Mapping-Tools>. Accessed 4 May 2023
- Helmi H, Basri H, Sufardi S, Helmi H (2019) Flood vulnerability level analysis as a hydrological disaster mitigation effort in Krueng Jreue Sub-Watershed, Aceh Besar Indonesia. *J Disaster Risk Stud* 11:737. <https://doi.org/10.4102/jamba.v11i1.737>
- Horton RE (1932) Drainage-basin characteristics. *Trans Am Geophys Union* 13:350–361. <https://doi.org/10.1029/TR013i001p00350>
- Horton RE (1945) Erosional development of streams and their drainage basins; hydrophysical approach to quantitative morphology. *GSA Bull* 56:275–370
- Jenson SK, Domingue JO (1988) Extracting topographic structure from digital elevation data for geographic information-system analysis. *Photogramm Eng Remote Sens* 54:1593–1600
- Joji VS, Nair ASK, Baiju KV (2013) Drainage basin delineation and quantitative analysis of Panamaram watershed of Kabani river basin, Kerala using remote sensing and GIS. *J Geol Soc India* 82:368–378. <https://doi.org/10.1007/s12594-013-0164-x>
- Khalil R (2018) Flood risk code mapping using multi criteria assessment. *J Geogr Inf Syst* 10:686–698. <https://doi.org/10.4236/jgis.2018.106035>
- Lee KKF, Ling L, Yusop Z (2023) The revised curve number rainfall-runoff methodology for an improved runoff prediction. *Water (Basel)* 15:1503. <https://doi.org/10.3390/w15030491>
- Malecha ML, Woodruff SC, Berke PR (2021) Planning to exacerbate flooding: evaluating a Houston, Texas, network of plans in place during hurricane Harvey using a plan integration for resilience scorecard. *Nat Hazards Rev* 22:470. [https://doi.org/10.1061/\(asce\)nh.1527-6996.0000470](https://doi.org/10.1061/(asce)nh.1527-6996.0000470)
- Mansour MM, Nasr M, Fujii M, et al (2023) Evaluation of a Reliable Method for Flash Flood Hazard Mapping in Arid Regions: A Case Study of the Gulf of Suez, Egypt. In: Chen X (ed) *Proceedings of the 2022 12th International Conference on Environment Science and Engineering (ICESE 2022)*. Springer Nature Singapore, Singapore, pp 103–117

- Manzoor Z, Ehsan M, Khan MB et al (2022) Floods and flood management and its socio-economic impact on Pakistan: a review of the empirical literature. *Front Environ Sci* 10:2480
- Mashaly J, Ghoneim E (2018) Flash flood hazard using optical, radar, and stereo-pair derived DEM: eastern desert Egtpt. *Remote Sens (Basel)* 10:10081204. <https://doi.org/10.3390/rs10081204>
- Masroor M, Sajjad H, Rehman S et al (2022) Analysing the relationship between drought and soil erosion using vegetation health index and RUSLE models in Godavari middle sub-basin. *India Geosci Front* 13:101312. <https://doi.org/10.1016/j.gsf.2021.101312>
- Miller VC (1953) A quantitative geomorphic study of drainage basin characteristics in the clinch mountain area. Columbia Univ New York, New York, Virginia and Tennessee
- Ministry of Water Resources and Irrigation (2017) The national water resources plan 2017–2030–2037 Summary
- Moawad MB, Abdel Aziz AO, Mamtimin B (2016) Flash floods in the Sahara: a case study for the 28 January 2013 flood in Qena Egypt. *Geomatics, Natural Hazards and Risk* 7:215–236. <https://doi.org/10.1080/19475705.2014.885467>
- Moglen GE, Eltahir EAB, Bras RL (1998) On the sensitivity of drainage density to climate change. *Water Resour Res* 34:855–862. <https://doi.org/10.1029/97WR02709>
- Mohamed SA (2019) Application of satellite image processing and GIS-Spatial modeling for mapping urban areas prone to flash floods in Qena governorate Egypt. *J African Earth Sci* 158:015. <https://doi.org/10.1016/j.jafrearsci.2019.05.015>
- Mohamed H, Abozeid G, Shehata S, Mohamed E (2021) Hydrological parameters affecting flash floods: case study Wadi Al-Baroud El-Abiad, Safaga City, red sea governorate. *Aswan Univ J Environ Stud* 2:42–56. <https://doi.org/10.21608/aujes.2021.149766>
- Moore DS, Notz WI, Fligner MA (2013) The basic practice of statistics, 6th edn. W. H Freeman and Company, New York
- Mudashiru RB, Sabtu N, Abustan I, Balogun W (2021) Flood hazard mapping methods: a review. *J Hydrol (amst)* 603:126846. <https://doi.org/10.1016/j.jhydrol.2021.126846>
- Nasr A, Abdelkareem M, Moubark K (2022) Integration of remote sensing and GIS for mapping flash flood hazards, Wadi Queih Egypt. *SVU-Int J Agric Sci* 4:197–206. <https://doi.org/10.21608/svuijas.2023.186199.1264>
- National Centers for Environmental Information (2020) Precipitation - PERSIANN CDR. <https://www.ncei.noaa.gov/products/climate-data-records/precipitation-persiann>. Accessed 3 Nov 2023
- Natsios A (2018) Hurricane Harvey: Texas at risk
- Obeidat M, Awawdeh M, Al-Hantouli F (2021) Morphometric analysis and prioritisation of watersheds for flood risk management in Wadi Easal Basin (WEB), Jordan, using geospatial technologies. *J Flood Risk Manag* 14:12711. <https://doi.org/10.1111/jfr3.12711>
- Ogarekpe NM, Obio EA, Tenebe IT et al (2020) Flood vulnerability assessment of the upper Cross River basin using morphometric analysis. *Geomat Nat Haz Risk* 11:1378–1403. <https://doi.org/10.1080/19475705.2020.1785954>
- Olsson L, Barbosa H, Bhadwal S et al (2019) Land degradation. *Climate Change and Land*. Cambridge University Press, Cambridge, pp 345–436
- Omran A, Schroeder D, El-Rayes A, Griesh M helmi (2011) Flood hazard assessment in Wadi Dahab, Egypt based on basin Morphometry using GIS techniques. In: Car A, Griesebner G, Strobl J (Eds): *Geospatial crossroads @ GI_Forum '11*. Herbert Wichmann Verlag, VDE VERLAG GMBH, Berlin/Offenbach
- Potter KW, Faulkner EB (1987) Catchment response time as a predictor of flood Quantiles. *JAWRA J Am Water Resour Assoc* 23:857–861. <https://doi.org/10.1111/j.1752-1688.1987.tb02962.x>
- ArcGIS Pro (2021) About ArcGIS Pro. <https://pro.arcgis.com/en/pro-app/2.9/get-started/get-started.htm>. Accessed 7 Mar 2023
- ArcGIS Pro (2023) What is model builder? <https://pro.arcgis.com/en/pro-app/latest/help/analysis/geoprocessing/modelbuilder/what-is-model-builder-htm>. Accessed 15 Nov 2023
- Redwan M, Abo Amra M, Abdelmoneim AA, Youssef AM (2021) Assessment of flood hazard west of sohag governorate Egypt. *Sohag J Sci* 6:1–8. <https://doi.org/10.21608/sjsoci.2021.233179>
- Saber M, Abdrabo KI, Habiba OM et al (2020) Impacts of triple factors on flash flood vulnerability in Egypt: urban growth, extreme climate, and mismanagement. *Geosciences (Switzerland)* 10:10010024. <https://doi.org/10.3390/geosciences10010024>
- Saleh A (2017) Developing a multi-criteria risk assessment tool for sizing flood protection structures faculty of engineering. Ain Shams University, Cairo
- Schumm SA (1956) Evolution of drainage systems and slopes in badlands at Perth Amboy, New Jersey. *GSA Bull* 67:597–646. [https://doi.org/10.1130/0016-7606\(1956\)67\[597:EODSAS\]2.0.CO;2](https://doi.org/10.1130/0016-7606(1956)67[597:EODSAS]2.0.CO;2)
- Seaborn (2022) seaborn: statistical data visualization. <https://seaborn.pydata.org/>. Accessed 5 Sep 2023
- Sherief YSY (2008) Flash floods and their effects on the development in El-QAA plain area in South Sinai, Egypt a study in applied geomorphology using GIS and remote sensing. Johannes Gutenberg University Mainz, Mainz
- Soil & Water Assessment Tool (2014) CFSR global weather data for SWAT 1979-2014 | SWAT | Soil & water assessment tool. <https://swat.tamu.edu/data/cfsr>. Accessed 30 Sep 2022
- Strahler AN (1957) Quantitative analysis of watershed geomorphology. *EOS Trans Am Geophys Union* 38:913–920. <https://doi.org/10.1029/TR038i006p00913>
- Taha MMN, Elbarbary SM, Naguib DM, El-Shamy IZ (2017) Flash flood hazard zonation based on basin morphometry using remote sensing and GIS techniques: a case study of Wadi Qena basin, Eastern Desert. *Egypt Remote Sens Appl* 8:157–167. <https://doi.org/10.1016/j.rsase.2017.08.007>
- Tesema TA (2021) Impact of identical digital elevation model resolution and sources on morphometric parameters of Tena watershed. Ethiopia. *Heliyon* 7:e08345. <https://doi.org/10.1016/j.heliyon.2021.e08345>
- The Red Sea Governorate (2023) Safaga. <http://www.redsea.gov.eg/t/News/Safaga/safagahistory.aspx>. Accessed 18 Aug 2023
- The World Bank Group (2021) Climate Risk Profile: Egypt
- United States Geological Survey (2018) USGS EROS archive - digital elevation - shuttle radar topography mission (SRTM) 1 arc-second global | U.S. Geological Survey. https://www.usgs.gov/centers/eros/science/usgs-eros-archive-digital-elevation-shuttle-radar-topography-mission-srtm-1?qt-science_center_objects=0#qt-science_center_objects. Accessed 30 Sep 2022
- United States Geological Survey (2021) EarthExplorer. <https://earthexplorer.usgs.gov/>. Accessed 30 Sep 2022
- US Army Corps of Engineers Hydrologic Engineering Center (2020) HEC-HMS. <https://www.hec.usace.army.mil/software/hec-hms/default.aspx>. Accessed 7 Mar 2023
- Youssef AM, Pradhan B, Gaber AFD, Buchroithner MF (2009) Geomorphological hazard analysis along the Egyptian Red Sea coast between Safaga and Quseir. *Nat Hazards Earth Syst Sci* 9:751–766. <https://doi.org/10.5194/nhess-9-751-2009>
- Youssef AM, Hegab M (2019) 10-Flood-hazard assessment modeling using multicriteria analysis and GIS: a case study—Ras Gharib Area, Egypt. In: *spatial modeling in gis and r for earth and environmental sciences*. pp 229–257
- Zaid SM (2009) Potential of flash flooding of the drainage basin of Quseir area a risk evaluation
- Zhang Y, Wang Y, Chen Y et al (2021) Projection of changes in flash flood occurrence under climate change at tourist attractions. *J Hydrol (Amst)* 595:126039. <https://doi.org/10.1016/j.jhydrol.2021.126039>